A Tutorial on Control Design of Hard Disk Drive Self-Servo Track Writing

Jianbin Nie and Roberto Horowitz

***Abstract*—In the recent five decades, magnetic hard disk drives have been playing an important role in the development of digital technology. The increasing areal density has provided a lot of challenges for the hard disk drive servo control. During the HDD servos, one of the most important parts is servo pattern which is utilized to generate position feedback signals. Thus, the accuracy and precision of servo patterns written by servo track writing process must be emphasized in order to increase the storage density. The concentric self-servo track writing has been proposed to improve the quality of servo patterns and save the cost of servo track writing. In this paper, we offer a tutorial on the control design of the self-servo track writing process. Besides, this paper presents two novel controller synthesis methodologies for performing concentric self-servo track using a feedforward control structure. In the first methodology, it is assumed that a conventional track-following causal controller has been designed and a non-causal feedforward controller, which utilizes the stored error signal from writing the previous track, is designed using standard H_∞ control synthesis techniques, in order to prevent the track errors from previous tracks from propagating and achieve good disturbance attenuation. In the second methodology, both the track-following feedback controller and the feedforward controller are simultaneously designed via a mixed H_2/H_∞ control scheme, which involves the solution of a set of linear matrix inequalities and achieves good disturbance attenuation while preventing the propagation of track errors from the previous tracks. Simulation results confirm that the two proposed control synthesis methodologies prevent error propagation from the previously written tracks and significantly improve self-servo track writing performance.**

I. Introduction

A. Hard disk drive servo systems

Since the commercial usage of magnetic disk drives began in 1956 [1], the hard disk drive (HDD) has been playing an important role in the modern era of digital technology. A hard disk drive is a non-volatile storage device that stores digitally encoded data on rotating rigid platters with magnetic surfaces. As a result, the problem of accessing data on the rapidly rotating disk media has provided a wealth of control challenges. For the operation of accessing data, a typical modern HDD has the basic components [2] as illustrated in Fig. 1. Data are recorded on concentric tracks on the disk which is rotated by the spindle motor. The magnetic heads attached onto the slider read and write data from and to the disk. The slider is bonded to the so-called suspension of the actuator arm which pivots about a ball bearing. Thus, as rotating the actuator of the voice coil motor (VCM), we can position the read/write head onto the desired tracks.

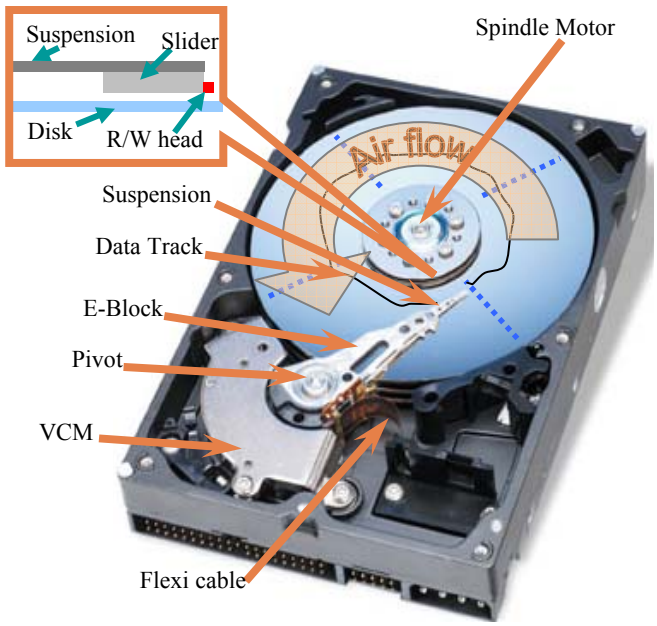

Fig. 1 Schematic of a typical modern hard disk drive.

According to the features of accessing data on disk, HDD servo systems mainly involve three kinds of control tasks [3]: track-seeking control, track-following control, and setting control. The head positioning servomechanism moves the read/write head as fast as possible from one track to another when asked by the host system (Track-seeking control). Once the head reaches the target track, it is regulated over the track so that the head can follows the track as precisely as possible during the operation of reading or writing data (Track-following control). Smooth settling, i.e. transition between the track seeking and track following modes without any jerk should be also emphasized in HDD servos.

Because of the increasing demand of magnetic disk storage devices and the improvement of HDD technology, the storage capacity of HDDs is phenomenally increasing. Meanwhile, in order to meet such demand, the areal density of HDDs must be increased so that the dimensions of HDDs could be maintained or even reduced. The trend of the areal density increase is demonstrated in Fig. 2. The first hard disk drive

Manuscript received September 15, 2009

This work was supported in part by the Information Storage Industry Consortium and the Computer Mechanics Laboratory at UC Berkeley.

J. Nie and R. Horowitz are with the Department of Mechanical Engineering, University of California, Berkeley (email: njbin@berkeley.edu, horowitz@me.berkeley.edu).

(RAMAC) supported an areal density of 2000 bits/^{in2} only. Today, the target for the storage density is 4 Tbit/in^2, which is an increase by a factor of 200 million. By considering that there exist significant disturbances [4] from windage caused by airflow, track runout due to disk vibrations and spindle vibrations, and measurement noise due to demodulation noises and electronic noises, to achieve the current target is really challenging. In order to accomplish the higher storage density, a lot of novel techniques, such as dual-stage actuation [5] and instrumented suspension [6], have been proposed from the part of HDD servo control. For dual-stage actuation, a second micro-actuator [7] is added to increase the system bandwidth so that the disturbances can be furthermore attenuated. The approach of instrumented suspension involves adding additional sensors to suspension, allowing for better control through the resonances of the actuator [8].

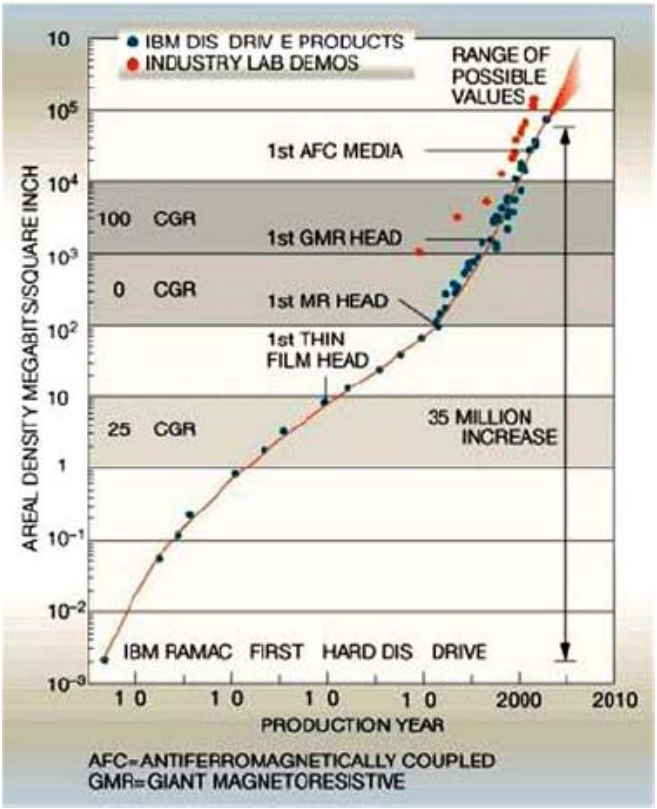

Fig. 2 The growth of areal density. The figure is from [9].

As feedback control systems, HDD servo systems require the sensing of read/write head position. Modern HDDs generate position feedback signals from special magnetic patterns called servo patterns which are written in designated areas on the disk surface known as servo sectors. The generated feedback signals are called position error signals (PES). Besides, the servo sectors are created at the time of manufacturing and are never overwritten or erased. Then, the closed-loop servomechanism decodes the position information written in these sectors to accomplish adequate control tasks.

B. Servo track writing

As discussed in the previous section, the servo patterns, used to generate position feedback signals, must be pre-created. The process of writing servo patterns onto the disk surface at specific locations of servo sectors is known as servo track writing (STW). Since the written servo patterns are utilized to generate the feedback signals for the read/write head position, the accuracy and precision of servo track writing process plays an important role in making the continuously growing trend of track density a reality. For the desired accuracy, there are two critical control problems [9] in the STW process:

1) All patterns required to define the tracks and sectors must be placed in a concentric fashion. Any disturbance and eccentricity present during the process will appear as written-in repeatable runout (RRO) which may degrade the servo performances of the three control tasks.
2) The servo sectors of any track must be precisely aligned with the servo sectors of adjacent tracks. The misalignment results in non-equidistant PES sampling intervals.

In order to improve the precision of servo patterns, the STW process also requires kind of position reference to form a feedback closed-loop control system. According to the different methods used to provide the reference, there have been proposed different kinds of servo track writing techniques, such as conventional servo track writing [10], concentric based self-servo track writing [11], and spiral self-servo track writing [12].

Conventionally, servo patterns are written by costly dedicated servowriting equipment [10] external to disk drives. For example, a laser-guided push-pin mechanism consists of an optical position sensor and controls the position of the write head so that concentric tracks can be created. Besides, in order to precisely align servo patterns along the disk's circumference, a clock track must be firstly written onto the disk and an external clock head is required to read back the timing information from the clock track. Consequentially, the conventional servo writing process needs openings in the drive enclosure to make the external equipment accessible to the media and actuator of the HDD. Moreover, in order to avoid the contamination, it is necessary to carry out the conventional servo writing process in a very clean environment. Besides, as the track density is increasing, the conventional STW using the external equipment is more time-consuming. In order to overcome these drawbacks, the methodologies of self-servo track writing have been developed.

The self-servo track writing (SSTW) process utilizes the HDD's own reading and writing heads and servo system to write servo patterns without using the external equipment. Thus, the clean room environment is not necessary for the SSTW process, which saves the cost of servo track writing. Besides, with the HDD's own servo system, a self servowriting loop is able to furthermore suppress vibrations

via active control, which means the SSTW can improve the quality of servowriting. Currently, there are two kinds of popular SSTW methodologies, i.e. concentric SSTW and spiral SSTW. The concentric SSTW process utilizes the pre-written concentric tracks to write the rest of concentric tracks. And the details of this methodology will be presented in the next section. The spiral SSTW process writes concentric product servo patterns based on the pre-written spirals tracks. The spiral tracks are written by using an external spiral writer, which is less expensive and less time-consuming than the conventional servo track writing process. However, such methodology involves a significant problem that the time of writing final servo patterns may coincide with the time of reading spiral servo information when servoing on spiral servo patterns to write final concentric servo patterns [12]. This conflict, caused by the fact that a HDD servo system can not read and write at the same time, is referred as a "collision" of the spiral servo information with the final servo pattern. As a result, the collision makes the feedback signal unavailable, which results in irregular sampling rate. Currently, the irregular sampling rate is a big challenge for the control design of spiral SSTW systems.

C. Concentric self-servo track writing

As discussed in the previous section, the increasing areal density requires the increasing track density. In order to reduce track misregistration and increase track density, it is necessary to improve the precision of the servo pattern writing process. Concentric self-servo track writing (SSTW) is an alternative method of writing servo patterns using the HDD's own reading and writing heads and servo system, in order to save the process cost and improve the servowriting quality.

The function block diagram for the concentric SSTW process is shown in Fig. 3. During the process, the timing and radial information are obtained from the previously written track using the read head, while timing and radial positioning servo patterns for the current track are being written using the write head. With the timing and radial information generated by the read head from the previously written track, a complete SSTW system includes two control loops [9], radial position control loop and timing control loop. By controlling the radial position of the write head with the help of controlling the actuator voice coil motor by using the generated position error signals from the previously written tracks as feedback signals, the radial position control loop ensures that all servo patterns used to define the tracks and servo sectors are placed in a concentric fashion. Meanwhile, with the help of the phase lock loop (PLL), the timing control loop servo sectors of any track are required to be precisely aligned along the disk's circumference. The control design of these two control loops is similar to each other and we just focus on the servo control of the radial position control loop in this paper.

Furthermore, the process of the concentric self-servo track writing is shown in Fig. 4 and it generally involves the following steps [11]:

1) Write some tracks at least one track called the seed tracks by using conventional servowriting methodologies. The seed tracks can be pre-written on disks before the disks are assembled in the HDD.
2) Assume a constant read-head-write-head offset of one track width [13]. The read head reads back the timing and radial information from the previously written seed track and track follows the seed track, while the write head writes actual servo patterns including the timing and radial information for the current track based on the readback signals.
3) Use the track written in step 2) as a seed track and go back to step 2) until all tracks are written.

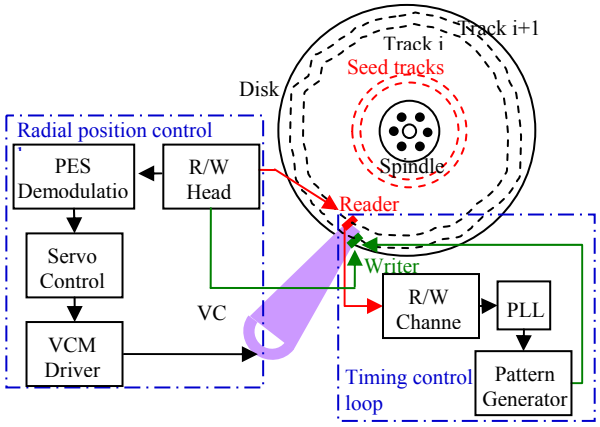

Fig. 3 Function block diagram of concentric SSTW servo systems.

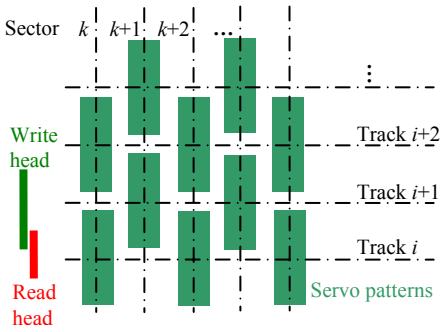

Fig. 4 Modeling of concentric SSTW servo systems.

Consequentially, the external equipment is no longer needed in the servo-pattern writing and thus the servo track writing does not have to be carried out in any clean room environment. Besides, by avoiding using the external servowriters, the concentric self-servo track writing process is much less time-consuming than the conventional servo writing process for the high density of servo tracks.

The paper is organized as follows. Section II provides control basics for SSTW servo systems. Section III describes the non-causal feedforward control design by using standard H_∞ control. In Section IV, the analytical expression for the power spectrum density of track errors is derived. Section V

presents the design of feedback and feedforward controllers by using a mixed H_2/H_∞ synthesis. Simulation results are provided in Section VI. Finally, conclusions are given in Section VII.

II. CONTROL BASICS FOR CONCENTRIC SSTW SYSTMES

A. Modeling of concentric SSTW systems

As discussed in the previous section, the concentric self-servo track writing systems track follow the previously written track, while writing the servo patterns for the current track. The servo writing of every individual track is just a regular track-following mode. However, the track errors from the previous track will be transmitted to the current track. Thus, the concentric SSTW servo system can be modeled as Fig. 5. The system includes a feedback loop with the VCM as plant $P(z)$ and the feedback controller $C(z)$. In Fig. 5, i and k denote the track index and servo sector index respectively, while $\Delta y_i(k)$, $w_i(k)$, $r_i(k)$ and $n_i(k)$ denote the track error, windage, track runout, and measurement noise, respectively, at the position of track i and servo sector k. Here, windage and measurement noise are modeled as white noises with the variance σ_w^2 and σ_n^2 respectively, while the track runout caused by disk vibrations and spindle vibrations is modeled as a color noise generated by feeding a white noise d_r input to the filter $G_r(z)$. The disturbance models σ_w^2, σ_n^2 and $G_r(z)$ can be identified from the closed-loop PES power spectrum density with the power spectrum density decomposition techniques [14].

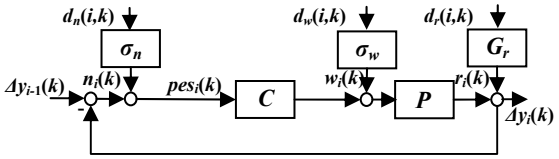

Fig. 5 Modeling of concentric SSTW servo systems.

B. Control design of concentric SSTW servo systems

Although the concentric SSTW can improve the quality of servo track writing and save the process cost and time, several challenges also arise with such servo track writing process such as the fact that radial position errors from the previous track can propagate into the currently written track. This radial positioning error propagation can lead to instability unless it is contained by guaranteeing that the magnitude for the error propagation term is sufficiently attenuated. Meanwhile, for each individual track, the SSTW servo control is just a track-following control mode which is required to attenuate the disturbances caused by windage, track runout, disk vibrations and measurement noise. Therefore, the major challenge for the concentric SSTW servo control is to achieve appropriate disturbance attenuation and the containment of the track error propagation simultaneously. In order to overcome such challenge, several control design methodologies have been proposed, for example, the control design by using 2-Dimensional Roesser model [15] and the control design based on a feedforward control structure [16].

For the control synthesis using 2-D Roesser models, the SSTW servo systems are modeled as the following 2-D model:

$$\begin{cases} \begin{bmatrix} x^h(i+1,k) \\ x^v(i,k+1) \end{bmatrix} = A \begin{bmatrix} x^h(i,k) \\ x^v(i,k) \end{bmatrix} + B_1 d(i,k) + B_2 u(i,k) \\ \Delta y(i,k) = C_1 \begin{bmatrix} x^h(i,k) \\ x^v(i,k) \end{bmatrix} + D_{11} d(i,k) \\ pes(i,k) = C_2 \begin{bmatrix} x^h(i,k) \\ x^v(i,k) \end{bmatrix} + D_{21} d(i,k) \end{cases}$$

where $d(i,k) = \begin{bmatrix} d_w(i,k) & d_r(i,k) & d_n(i,k) \end{bmatrix}^T$. Then the 2-Dimensional control theory such as 2-D H_2 control [17], 2-D H_∞ control [18] and 2-D robust mixed H_2/ H_∞ control [19] can be utilized to design a 2-D feedback controller C for SSTW servo systems shown in Fig. 5. However, all of the control techniques in [17-19] are just formulated to satisfy a sufficient rather than a sufficient and necessary condition by making some matrices be block diagonal in order to transfer the optimization to the corresponding convex optimization in the form of linear matrix inequalities (LMI). Moreover, these designed controllers are usually complicated and it is quite difficult to comprehend them.

Alternatively, the control design based on the feedfoward control structure was proposed. The commonly used control architecture with the feedforward control is illustrated in Fig. 6. This control synthesis involves a feedback controller $C(z)$ to attenuate disturbances and a feedfoward controller $F(z)$ to contain the error propagation from the previously written tracks. The feedback controller track follows the previously written track by generating the feedback signal $PES_i(k)$ from the servo patterns on this track, while the feedforward controller contains the track error propagation by using the error signal $e_{i-1}(k)$. More features of such control design will be discussed in the following section. Based on the feedfward control structure, several novel control design techniques have been developed for SSTW servo systems in [20-24]. All of these design techniques in [20-24] involve two design steps that a standard track-following controller $C(z)$ with appropriate disturbance attenuation is firstly designed and then a feedforward controller $F(z)$ is designed to produce a satisfactory track-error propagation containment. In [20], the authors compared the optimal H_2 control with the proportional-integral-derivative (PID) control for the track-following control design and concluded that the former control design is able to achieve the better performance than the latter one. In [24], the authors utilized the estimation of the head position to design the feedforward control. In [21], [22] and [23], the feedforward control based on iterative learning control is designed in the lifted domain assuming zero initial conditions at the beginning of each track servo writing stage and the existence of finite impulse-response (FIR) representations for the servo's sensitivity and

complimentary sensitivity functions. However, we note that these assumptions are not strictly true for real HDDs.

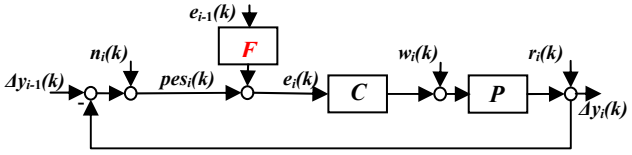

Fig. 6 Feedforward control structure based SSTW system.

In this paper, we present two novel control synthesis methodologies for performing concentric self-servo track writing in hard disk drives using the feedforward control structure illustrated in Fig. 6. In the first methodology, a good track-following controller is pre-designed as the feedback controller $C(z)$ and then a non-causal feedforward controller, which utilizes the stored error signal [21] from writing the previous track, is designed by using standard H_∞ control techniques. These H_∞ control synthesis techniques are used to guarantee the attenuation of track errors from the previous tracks, while achieving sufficient disturbance attenuation. In the second methodology, an analytic expression for the power spectrum density of track errors is derived. The expression is subsequently used to formulate the simultaneous design of both a feedback and a feedforward controller, using a mixed H_2/H_∞ control scheme, which ensures the containment of the error propagation and the achievement of good disturbance attenuation and is solved via the solution of a set of LMIs. Neither of these techniques utilizes the simplifying assumptions in [21] and [22]. Simulation results using the HDD benchmark problem developed in [25] show that the controllers synthesized using the proposed schemes outperform the controllers synthesized by the techniques in [21], and offer levels of performance that are comparable to the 2-dimensional H_2 control technique in [17] while having a simpler structure.

III. Non-causal Feedforward Control Design via H_∞ Control

A. Feedforward-control structure based SSTW system

As discussed in the previous section, the feedback control $C(z)$ must be pre-designed to achieve good disturbance attenuation for the feedforward-control-structure based concentric SSTW systems illustrated in Fig. 6. Here, the optimal H_2 control design methodology in [26] is utilized to design $C(z)$. Such control synthesis produces robust stability by tuning a control input weighting function while achieving adequately good performance of disturbance suppression.

Based on the block diagram in Fig. 6, we can get the following recursive expression for track errors:

$$\Delta y_i(k) = G_1(z)\Delta y_{i-1}(k) + T(z)n_i(k) + S(z)d_i(k) - S(z)F(z)d_{i-1}(k) \quad (1)$$

where $T(z) = \dfrac{C(z)P(z)}{1+C(z)P(z)}$, $S(z) = \dfrac{1}{1+C(z)P(z)}$, $d_i(k) = P(z)w_i(k) + r_i(k)$, and $G_1(z) = \dfrac{C(z)P(z)+F(z)}{1+C(z)P(z)}$.

Notice that $G_1(z)$ turns out to be the key transfer function relating the previous and the current track errors.

B. Non-causal feedforward control design

Since the feedforward controller $F(z)$ utilizes the error signal $e_{i-1}(k)$, which can be stored when writing the previous track, and hence the entire $e_{i-1}(k)$ sequence in (k) is available when writing the current track, a non-causal feedforward controller $F(z)$ is feasible for the control structure in Fig. 6. Besides, in order to contain the error propagation, the designed controllers are required to satisfy $\|G_1(e^{j\omega})\|_\infty<1$. Furthermore, in order to make the error propagation converge as quickly as possible, we want $\|G_1(e^{j\omega})\|_\infty$ to be sufficiently small. From (1), we learn that the current track error is also affected by the disturbances from the previous tracks. In order not to degrade the disturbance attenuation performance of the track-following controller $C(z)$, the magnitude of the filter $F(z)$ needs to be sufficiently small as well. In all, the feedforward control $F(z)$ is desired to achieve the following target:

$$\begin{cases} \|G_1(z)\|_\infty : \text{sufficiently small and } <1 \\ \|F(z)\|_\infty : \text{sufficiently small} \end{cases} \quad (2)$$

As a consequence, we consider the following optimization:

$$\min_{F(z)} \left\| \begin{bmatrix} G_1(z) & w_{t1}F(z) \end{bmatrix} \right\|_\infty \quad (3)$$

where w_{t1} is a weighting value to be tuned to achieve the target in (2). The optimization in (3) is a standard H_∞ control design [27] and can be easily solved. However, the solution to (3) can only produce a causal compensator $F(z)$. Obviously, a smaller objective value may be achieved if $F(z)$ is allowed to be non-causal. In order to design a non-causal filter $F(z)$, by considering the fact that introducing an input delay will not affect the H_∞ norm of LTI systems, we have:

$$\left\| \begin{bmatrix} G_1(z) & w_{t1}F(z) \end{bmatrix} \right\|_\infty = \left\| \begin{bmatrix} z^{-n_d}G_1(z) & w_{t1}z^{-n_d}F(z) \end{bmatrix} \right\|_\infty = \left\| \begin{bmatrix} \dfrac{z^{-n_d}P(z)C(z)+\tilde{F}(z)}{1+P(z)C(z)} & w_{t1}\tilde{F}(z) \end{bmatrix} \right\|_\infty \quad (4)$$

where $F(z) = z^{n_d}\tilde{F}(z)$ and n_d is a positive integer. Thus, the optimization in (3) can be transformed into the following optimization:

$$\min_{\tilde{F}(z)} \left\| \begin{bmatrix} \dfrac{z^{-n_d}P(z)C(z)+\tilde{F}(z)}{1+P(z)C(z)} & w_{t1}\tilde{F}(z) \end{bmatrix} \right\|_\infty \quad (5)$$

Then, it is necessary to construct an LTI system to formulate the H_∞ control problem in (5).

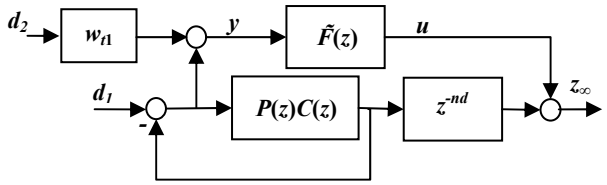

Fig. 7 Block diagram for the interpretation of H_∞ norm.

By considering the block diagram in Fig. 7, we have $T_{z_\infty \leftarrow [d_1 \quad d_2]^T} = \begin{bmatrix} \dfrac{z^{-n_d}P(z)C(z)+\tilde{F}(z)}{1+P(z)C(z)} & w_{t1}\tilde{F}(z) \end{bmatrix}^T$. Thus, the optimization in (5) can be interpreted as the H_∞ control problem for the linear fractional transformation (LFT) in Fig. 8 to minimize $\left\| T_{z_\infty \leftarrow d_\infty} \right\|_\infty$. In Fig. 8, $G(z)$ is the transfer function matrix from $\begin{bmatrix} d_\infty^T & u \end{bmatrix}^T$ to $\begin{bmatrix} z_\infty^T & y \end{bmatrix}^T$.

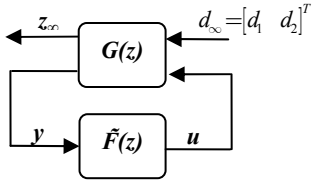

Fig. 8 LFT for the H_∞ control design problem.

Once the causal filter $\tilde{F}(z)$ is designed, the corresponding non-causal feedforward controller can be constructed from $F(z) = z^{n_d}\tilde{F}(z)$.

IV. Track Error Analysis for the Feedforward Control Based SSTW

A. Power spectrum density of track errors

As discussed in the previous section, the disturbances from writing the previous tracks definitely affect the current track writing. It is meaningful to investigate the relationship between the current track error and disturbances from writing the previous tracks so that the better control synthesis may be provided. In order to analyze the power spectrum density of track errors which will be discussed in detail later, we assume that the writing of servo patterns starts after the transition response disappears and all of N servo patterns on each track are written successively during one revolution of the disk. Then, based on the recursive form of track errors in (1), we have the following complete expression for track errors.

$$\begin{aligned}\Delta y_i(k) &= G_1^i \Delta y_0(k) + \sum_{l=1}^{i} G_1^{i-l} T n_l(k) + \sum_{l=1}^{i} G_1^{i-l} S d_l(k) - \sum_{l=1}^{i-1} G_1^{i-1-l} SF d_l(k)) \\ &= G_1^i \Delta y_0(k) + \sum_{l=1}^{i-1} G_1^{i-1-l} T\left[(T+SF) n_l(k) - S(1-F) d_l(k) \right] \\ &\quad + T n_i(k) + S d_i(k) \\ &= G_1^i \Delta y_0(k) + \sum_{l=1}^{i-1} G_1^{i-1-l} T\left[G_1 n_l(k) - S(1-F) d_l(k) \right] + T n_i(k) + S d_i(k)\end{aligned} \tag{6}$$

Furthermore, we assume that the seed track error Δy_0, measurement noises and disturbances are uncorrelated with each other and the track error on the seed track has a power spectrum density $\Phi_{\Delta y_0 \Delta y_0}(e^{j\omega})$. Moreover, measurement noises on different tracks are uncorrelated and have the same variance σ_n^2, while disturbances on different tracks are also uncorrelated and have the same power spectrum density $\Phi_{dd}(e^{j\omega})$. With these assumptions, we can get the following power spectrum density for the track error on track i:

$$\begin{aligned}\Phi_{\Delta y_i \Delta y_i}(e^{j\omega}) &= |G_1|^{2i} \Phi_{\Delta y_0 \Delta y_0} + \sum_{l=1}^{i-1} |G_1|^{2(i-l-1)} |T|^2 \left\{ |G_1|^2 \sigma_n^2 + |S|^2 |1-F|^2 \Phi_{dd} \right\} \\ &\quad + |T|^2 \sigma_n^2 + |S|^2 \Phi_{dd}\end{aligned} \tag{7}$$

When the track index i is quite large, $|G_1(e^{j\omega})|^{2i}$ will be closed to zero, since $\|G_1(e^{j\omega})\|_\infty < 1$. Then, for the large track index i, we have:

$$\Phi_{\Delta y_i \Delta y_i}(e^{j\omega}) = \frac{|T|^2}{1-|G_1|^2}\left\{ \sigma_n^2 + |\hat{F}|^2 \Phi_{dd}(e^{j\omega}) \right\} + |S|^2 \Phi_{dd}(e^{j\omega}) \tag{8}$$

where in order to conveniently synthesize the mixed H_2/H_∞ control, which will be discussed in Section IV, we utilize the parameterization $G_1(z) = 1 + \hat{F}(z)$ and $\hat{F}(z) = S(z)(1-F(z))$.

B. Discussion

From (8), we note that, in order to reduce track errors, not only a good track-following feedback controller is necessary, but also both $|G_1(e^{j\omega})|$ and $|\hat{F}(e^{j\omega})|$ should be sufficiently small. However, $|G_1(e^{j\omega})|$ and $|\hat{F}(e^{j\omega})|$ can not be small at the same time, since $G_1(z) = 1 + \hat{F}(z)$. Intuitively, in order to accomplish a good tracking performance, the H_2 norm of the transfer functions from disturbances to track errors must be minimized at the same time that an appropriately small $\|G_1(z)\|_\infty$ is guaranteed. This idea turns out to be a mixed H_2/H_∞ control problem, which will be discussed in next section.

V. The Design of Feedback and Feedforward Control by Using a Mixed H_2/H_∞ Synthensis

A. Problem formulation

As discussed in Section IV, (8) educes the idea of a mixed H_2/H_∞ control design in order to achieve a tracking good performance. Let's rewrite (8) as:

$$\Phi_{\Delta y_i \Delta y_i}(e^{j\omega}) = |T|^2 \left(\frac{\sigma_n^2}{1-|G_1|^2} \right) + |\hat{F}|^2 \left(\frac{|T|^2}{1-|G_1|^2} \Phi_{dd}(e^{j\omega}) \right) + |S|^2 \Phi_{dd}(e^{j\omega}) \tag{9}$$

Clearly, (9) demonstrates that the track error can considered as the output of the system $\bar{G}_2(z) = \begin{bmatrix} T(z) & \hat{F}(z) & S(z) \end{bmatrix}$ with the input of $\begin{bmatrix} \dfrac{n_i}{\left(1-|G_1(z)|^2\right)^{1/2}} & \dfrac{T(z)}{\left(1-|G_1(z)|^2\right)^{1/2}} \tilde{d}_i & d_i \end{bmatrix}^T$. Here, $\tilde{d}_i$ are artificial disturbances, which are uncorrelated with n_i and d_i and have the same power spectrum density as d_i. Since the weighting

functions $\frac{1}{\left(1-|G_1(z)|^2\right)^{1/2}}$ and $\frac{T(z)}{\left(1-|G_1(z)|^2\right)^{1/2}}$ for n_i and $\tilde{d}_i$ are not affine in $G_1(z)$ and $T(z)$, the two weighting functions are replaced by two weighting values w_{t2} and w_{t3} respectively, in order to conveniently construct a linear system to represent the transfer function matrix from the input $\begin{bmatrix} n_i & \tilde{d}_i & d_i \end{bmatrix}^T$ to Δy_i. By considering the system denoted in Fig. 9 where d_w, d_r, d_n, $\tilde{d}_w$, and $\tilde{d}_r$ are assumed to be uncorrelated white noises, we obtain the following expression for the power spectrum density of z_2:

$$\Phi_{z_2 z_2}(e^{j\omega}) = |T|^2 w_{t2}^2 \sigma_n^2 + \left|\hat{F}\right|^2 w_{t3}^2 \Phi_{\tilde{d}\tilde{d}}(e^{j\omega}) + |S|^2 \Phi_{dd}(e^{j\omega}) \quad (10)$$

Obviously, the power spectrum density of z_2 is similar to that of Δy_i except the replacement of the weighting functions in (9) with the corresponding weighting values in (10). Thus, with appropriate weighting values w_{t2} and w_{t3}, $\Phi_{\Delta y_i \Delta y_i}(e^{j\omega})$ can be approximated by $\Phi_{z_2 z_2}(e^{j\omega})$. As shown in Fig. 9, let $G_2(z) = \left[T_{z_2 \leftarrow \begin{bmatrix} d_w & d_r & d_n \end{bmatrix}^T} \quad w_{t3}\hat{F} * T_{\tilde{d} \leftarrow \begin{bmatrix} \tilde{d}_w & \tilde{d}_r \end{bmatrix}^T} \right]$ denote the transfer function matrix from $\begin{bmatrix} d_w & d_r & d_n & \tilde{d}_w & \tilde{d}_r \end{bmatrix}^T$ to z_2.

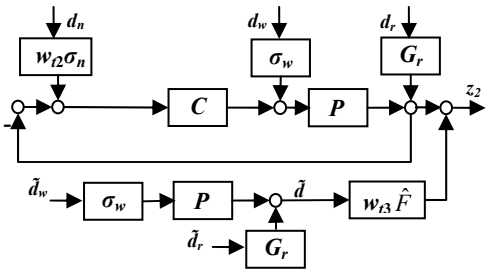

Fig. 9 Block diagram for the interpretation of $G_2(z)$.

Therefore, in order to accomplish good tracking error performance, we consider the following mixed H_2/H_∞ control to design $C(z)$ and $F(z)$ simultaneously.

$$\min_{C(z),F(z)} \left\|G_2(z)\right\|_2^2 \quad (11)$$
$$st \quad \left\|G_1(z)\right\|_\infty^2 < \gamma_0^2 < 1$$

where γ_0 is a given constant to guarantee good convergence for the track error propagation and a good attenuation for the disturbances from the previously written tracks.

B. Mixed H_2/H_∞ synthesis via LMIs

A number of techniques [28] have been developed to formulate the mixed H_2/H_∞ control problems such as (11), and the problems are frequently solved as solutions of linear matrix inequalities. However, in order to recover the convexity of the optimization, the solution approach through LMIs has to impose a constraint which brings significant conservatism to the optimal control, which is discussed in [26]. Moreover, the mixed H_2/H_∞ optimization in (11) is quite difficult to be solved, because both $G_1(z)$ and $G_2(z)$ not only include the feedback controller $C(z)$ but also the feedforward controller $F(z)$. In order to simplify the synthesis, we utilize the parameterization of $G_1(z) = 1 + \hat{F}(z)$. Then, with $\hat{F}(z) = S(z)(1 - F(z))$, the optimization in (11) can be reformulated as:

$$\min_{C(z),\hat{F}(z)} \left\|G_2(z)\right\|_2^2 \quad (12)$$
$$st \quad \left\|1 + \hat{F}(z)\right\|_\infty^2 < \gamma_0^2 < 1$$

The advantage of the formulation in (12) over the formulation in (11) is that the H_∞ norm constraint is independent of the feedback controller $C(z)$.

Obviously, $G_2(z)$ can be rewritten as $G_2(z) = \left[T_{z_2 \leftarrow \begin{bmatrix} d_w & d_r & d_n \end{bmatrix}^T} \quad 0 \quad 0 \right] + \hat{F} * \left[0 \quad 0 \quad 0 \quad w_{t3} T_{\tilde{d} \leftarrow \begin{bmatrix} \tilde{d}_w & \tilde{d}_r \end{bmatrix}^T} \right]$. Suppose we have the following state space realizations:

$$C(z) \sim \left[\begin{array}{c|c} A_C & B_C \\ \hline C_C & D_C \end{array}\right] \quad (13)$$

$$\left[T_{z_2 \leftarrow \begin{bmatrix} d_w & d_r & d_n \end{bmatrix}^T} \quad 0 \quad 0 \right] \sim \left[\begin{array}{c|c} A_{cl2} & B_{cl2} \\ \hline C_{cl2} & D_{cl2} \end{array}\right] \quad (14)$$

$$\left[0 \quad 0 \quad 0 \quad w_{t3} T_{\tilde{d} \leftarrow \begin{bmatrix} \tilde{d}_w & \tilde{d}_r \end{bmatrix}^T} \right] \sim \left[\begin{array}{c|c} A_d & B_d \\ \hline C_d & D_d \end{array}\right] \quad (15)$$

$$\hat{F} \sim \left[\begin{array}{c|c} A_{\hat{F}} & B_{\hat{F}} \\ \hline C_{\hat{F}} & D_{\hat{F}} \end{array}\right], G_1 = 1 + \hat{F} \sim \left[\begin{array}{c|c} A_{\hat{F}} & B_{\hat{F}} \\ \hline C_{\hat{F}} & 1 + D_{\hat{F}} \end{array}\right] \quad (16)$$

$$\hat{F} * \left[0 \quad 0 \quad 0 \quad w_{t3} T_{\tilde{d} \leftarrow \begin{bmatrix} \tilde{d}_w & \tilde{d}_r \end{bmatrix}^T} \right] \sim \left[\begin{array}{c|c} \bar{A}_f & \bar{B}_f \\ \hline \bar{C}_f & \bar{D}_f \end{array}\right]$$
$$= \left[\begin{array}{cc|c} A_d & 0 & B_d \\ B_{\hat{F}} C_d & A_{\hat{F}} & B_{\hat{F}} D_d \\ \hline D_{\hat{F}} C_d & C_{\hat{F}} & D_{\hat{F}} D_d \end{array}\right] \quad (17)$$

$$G_2 \sim \left[\begin{array}{c|c} \bar{A}_{cl2} & \bar{B}_{cl2} \\ \hline \bar{C}_{cl2} & \bar{D}_{cl2} \end{array}\right] = \left[\begin{array}{cc|c} A_{cl2} & 0 & B_{cl2} \\ 0 & \bar{A}_f & \bar{B}_f \\ \hline C_{cl2} & \bar{C}_f & D_{cl2} + \bar{D}_f \end{array}\right] \quad (18)$$

Then the optimization in (12) can be synthesized as the following optimization [9]:

$$\min_{A_C,B_C,C_C,D_C,C_{\hat{F}},D_{\hat{F}},X_1,X_2} trace(W)$$

$$st \begin{bmatrix} W & \bar{C}_{cl2} & \bar{D}_{cl2} \\ * & X_2 & 0 \\ * & * & I \end{bmatrix} \succ 0 \quad (19)$$

$$\begin{bmatrix} X_2 & X_2\bar{A}_{cl2} & P_2\bar{B}_{cl2} \\ * & X_2 & 0 \\ * & * & I \end{bmatrix} \succ 0 \quad (20)$$

$$\begin{bmatrix} X_1 & X_1A_{\hat{F}} & X_1B_{\hat{F}} & 0 \\ * & X_1 & 0 & C_{\hat{F}}^T \\ * & * & I & 1+D_{\hat{F}}^T \\ * & * & * & \gamma_0^2 I \end{bmatrix} \succ 0 \quad (21)$$

where the symbol "*" denotes the transpose of the corresponding element at its transposed position. Since both X_1 and X_2 are coupled with $A_{\hat{F}}$ and $B_{\hat{F}}$ in (21) and (20) respectively, the filter $\hat{F}(z)$ is chosen as an FIR filter, which means that $A_{\hat{F}}$ and $B_{\hat{F}}$ are known parameters and thus the inequality in (21) turns out to be a LMI. Moreover, in order to recover the convexity of (19) and (20) by a suitable nonlinear transformation [29], the matrix X_2 is chosen as $X_2 = diag\{X_{22}, X_{ff}\}$. As a result, the optimization involving (19), (20) and (21) is a convex optimization, which can be easily solved.

VI. Simulation Study

In order to evaluate the SSTW design methodologies presented in this paper, they will be tested via a simulation study that utilizes the benchmark model developed by the IEEJapan technical committee on Nano-Scale Servo (NSS) system [25]. This model was also utilized to test the SSTW design scheme presented in [21]. This benchmark model was originally developed to test track-following servos and must be modified to test servo systems for self-servo track writing control. For the simulated drive, the servo sector number N is equal to 220 and the disk speed is 7200 RPM. Thus, the sampling frequency for this drive is f_s = 220*7200/60 = 26400 Hz.

A. Control design results

A non-causal feedforward compensator $F(z)$ was first designed using the H_∞ design methodology presented in Section II, using an optimal H_2 track following compensator $C(z)$ with the weighting value w_{t1} = 0.16 and n_d = 7. The designed control system achieves $\|G_1(z)\|_\infty = 0.9781 < 1$ and $\|F(z)\|_\infty = 1.3633$. The corresponding frequency response plots for the designed $F(z)$, $(P(z)C(z)+F(z))/(1+P(z)C(z))$, $1/(1+P(z)C(z))$, and $F(z)/(1+P(z)C(z))$ are shown in Fig. 10.

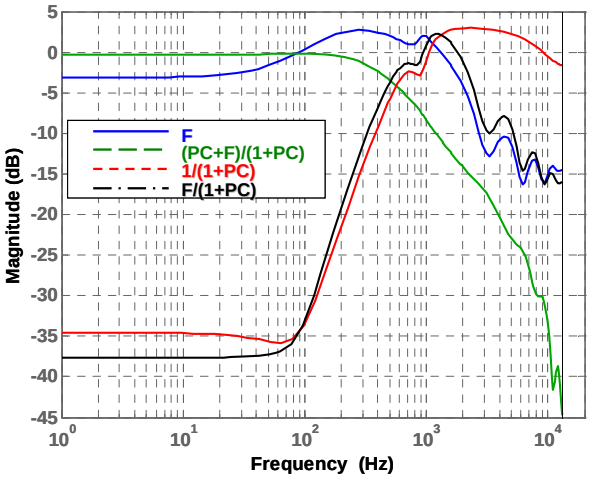

Fig. 10 Frequency responses for the non-causal feedforward control design via H_∞ control in Section II.

Subsequently, a feedforward compensator $F(z)$ constructed from the FIR filter $\hat{F}(z)$ and a feedback compensator $C(z)$ were simultaneously designed using the mixed H_2/H_∞ control synthesis methodology in Section IV. The designed control system achieves $\|G_1(z)\|_\infty = 0.9779$ with the tuning parameters w_{t2} = 4, w_{t3} = 4 and γ_0 = 0.98. The frequency response plots for the resulting controllers are shown in Fig. 11.

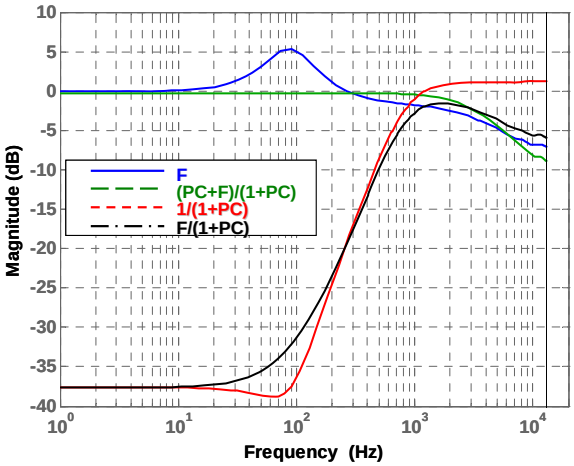

Fig. 11 Frequency responses for the feedback and feedforward control designs using the mixed H_2/H_∞ synthesis methodology in Section IV.

B. Time-domain simulation results

The benchmark problem in [25] was originally developed for evaluating track-following servos and must be modified to simulate a self-servo track writing system. In [25], the modeled sensor noise has a sigma value of 1.5% of track pitch; that of the track runout due to disk vibrations is 1.7% of track pitch; the contribution of the windage at *PES* has a sigma value of 12.2% track width. The track error for the seed track is assumed to be a sigma value of 14% track width. In the simulation, a total of 5000 servo tracks data was collected. In order to interpret the simulated results better, we also provide the time-domain simulation results for the 2-Dimensional H_2 SSTW synthesis technique presented in [17]. The sigma

values of the first 5000 self-servo written tracks for the proposed two methods in this paper and for the 2-D H_2 system are depicted in Fig. 12. Obviously, the track error propagation is well contained for the three design methodologies.

Meanwhile, by considering the relatively large variance of the seed track, we are also interested in checking how fast the transition response caused by the seed track can converge. The zoomed in figure for the transition response is illustrated in Fig. 13. The results demonstrate that the effect of the bad seed track on the subsequently written tracks by the proposed controllers disappears very quickly. Moreover, the simulation results show that the transition response can converge after about 15 tracks.

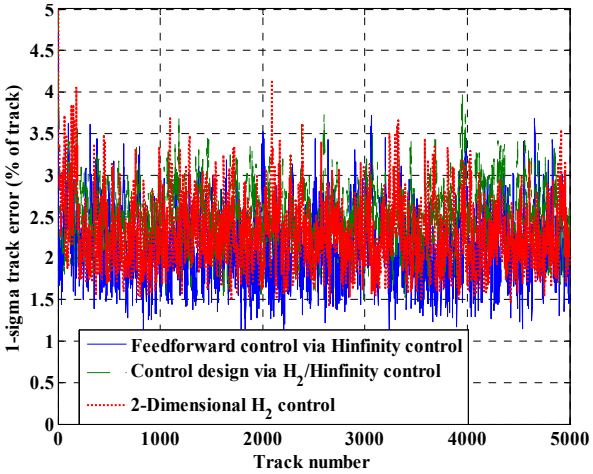

Fig. 12 Time domain simulation results for track errors. Since the performance of the control design via H_2/H_∞ is closed to that of 2-D H_2 control, the green line is almost covered by the red line.

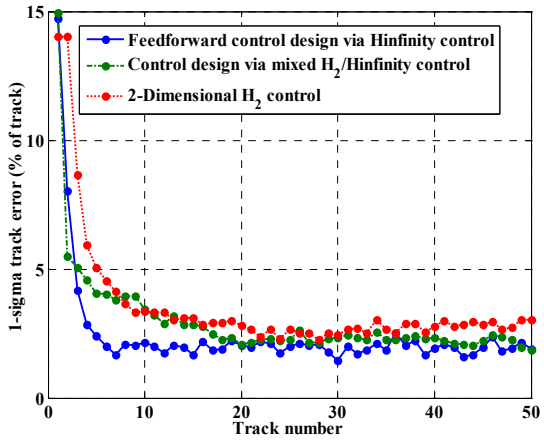

Fig. 13 Zoomed in Fig. 12 to check the transition response caused by the seed track.

We now consider another common performance index called AC squeeze in order to quantify the quality of written tracks. The AC squeeze for track i is defined as:

$$ACsqueeze_i = \min_{k\in[0,N-1]} \{1+\Delta y_i(k)-\Delta y_{i-1}(k)\} \qquad (22)$$

where track errors $\Delta y_i(k)$ and $\Delta y_{i-1}(k)$ are normalized by the track width. When the AC squeeze is too small, two adjacent tracks with narrow track spacing may interfere with each other and cause data corruption. The ideal value AC squeeze is 1 track width, which means the adjacent tracks are perfectly parallel to each other. The AC squeeze values for the simulated self-servo written tracks are shown in Fig. 14.

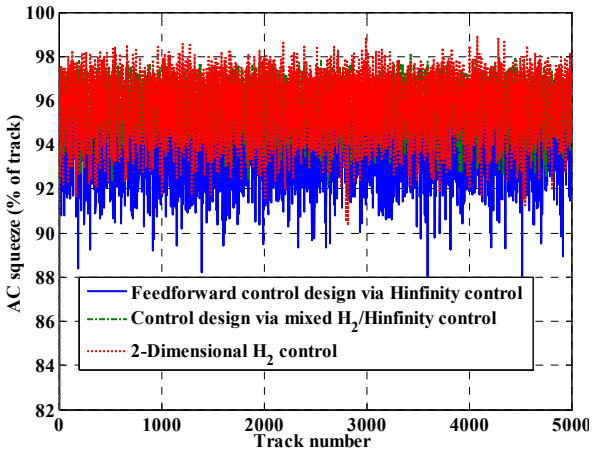

Fig. 14 Time domain simulation results for AC Squeeze. Since the performance of the control design via H_2/H_∞ is closed to that of 2-D H_2 control, the green line is almost covered by the red line.

Moreover, the resulting average values of $\sigma(\Delta y_i(k))$ and $ACsqueeze_i$ are presented in Table 1. Note that the non-causal feedforward control design through standard H_∞ control achieves the best performance for track errors, while the feedback and feedforward control designs by using the mixed H_2/H_∞ control accomplish the best AC squeeze.

In order to provide the better comparison for our proposed control synthesis, the simulation results reported in [21] by using the iterative learning control in lifted domain are also listed in Table 1. Obviously, the two proposed control design methodologies are able to improve both track errors and AC squeeze.

TABLE I SIMULATION RESULTS

	H_2 feedback control + non-causal feedforward control using H_∞ control	Feedback and feedforward control using mixed H_2/H_∞ control	2-D H_2 control	ILC in lifted domain [21]
Average of 1σ track error (% track)	2.11	2.50	2.27	2.88
Average of AC squeeze (% track)	94.0	96.0	95.8	88

VII. CONCLUSION

In this tutorial, we have examined the control design of concentric self-servo track writing. As the areal density of hard disk drives is creasing, the accuracy and precision of servo patterns written by servo track writing process to generate position feedback signals for HDD servo systems is

more and more important. The concentric self-servo track writing has been proposed to improve the quality of servo patterns and to save the cost of servo track writing. Besides, this paper discussed two novel controller synthesis methodologies for performing self-servo track writing in disk drives using a feedforward control structure. In the first methodology, it is assumed that a conventional track-following causal controller has been designed and a non-causal feedforward controller, which utilizes the stored error signal from writing the previous track, is designed using standard H_∞ control synthesis techniques, in order to prevent the track errors from previous tracks from propagating and to achieve good disturbance attenuation. In the second methodology, an analytic expression for the power spectrum density of track errors is derived. The expression is subsequently used to formulate the simultaneous design of both feedback and feedforward controllers, using a mixed H_2/H_∞ control scheme, which ensures the containment of the error propagation and the achievement of good disturbance attenuation and is solved via the solution of a set of LMIs. Neither of these techniques utilizes the simplifying assumptions in [21]. Simulation results using the HDD benchmark problem developed in [25] show that the controllers synthesized using the proposed schemes outperform the controllers synthesized by the techniques in [21], and offer levels of performances that are comparable with the 2-dimensional H_2 control technique in [17] while having a simpler structure. Moreover, the track error propagation converges very quickly although the seed track has a large track error.

ACKNOWLEDGMENT

The authors thank Western Digital Inc. for the motivation of this study.

REFERENCES

[1] L. Stevens, "Data storage on magnetic disks," *Magnetic Recording: The First 100 Years*. E. Daniel, C. Mee, and M. Clark, Eds. Piscataway, NJ: IEEE Press, pp. 270-299, 1997.

[2] B. Chen, T. Lee, and V. Venkataramanan, "Hard Disk Drive Servo Systems," Advances in Industrial Control Series, Springer, New Your, 2006.

[3] D. Abramovitch and G. Franklin, "A brief history of disk drive control," *IEEE Control Systems Magazine*, vol. 22, no. 3, pp. 28-42, 2002.

[4] E. Rich and D. Curran, "Major HDD TMR Sources and Projected Scaling with TPI," *IEEE Trans. On Magnetics*, vol. 35, no. 2, pp. 885-891, 1999.

[5] Y. Li and R. Horowitz, "Mechatronics of electrostatic microactuators for computer disk drive dual-stage servo systems," *IEEE/ASME Trans. Mechatronics*, vol. 6, pp. 988-992, 2001.

[6] S. Felix, J. Nie and R. Horowitz, "Enhanced vibration suppression in HDDs using instrumented suspensions," *IEEE Trans. On Magnetics*, vol. 45, no. 11, pp. 5118-5122, 2009.

[7] K. Oldham, X. Huang and R. Horowitz, "Design, Fabrication, and Control of a High-Aspect Ratio Microactuator for Vibration Suppression in a Hard Disk Drive," *Proceedings of the 16th IFAC Word Congress*, Prague, Czech Republic, July 4-8, 2005.

[8] X. Huang and R. Horowitz, "Robust controller design of a dual-stage disk drive servo system with an instrumented suspension," *IEEE Trans. On Magnetics*, vol. 41, no. 8, pp. 2406-2413, 2005.

[9] A. A. Mamun, G. Guo, and C. Bi, "Hard disk drive: mechatronics and control," *Automation and control engineering*, Boca Raton, FL, CRC Press, c2007.

[10] Y. Uematsu, M. Fukushi, and K. Taniguchi, "Development of the pushpin free STW," *IEEE Trans. On Magnetics*, vol. 37, no. 2, pp. 964-968, 2001.

[11] H. Ye, V. Sng, C. Du, J. Zhang, and G. Guo, "Radial error propagation issues in self servo track writing technology," *IEEE Trans. On Magnetics*, vol. 38, no. 5, pp. 2180-2182, 2002.

[12] D. Brunnett, Y. Sun, and L. Guo, "Method and apparatus for performing a self-servo write operation in a disk drive using spiral servo information," U.S. Patent 7230789B1, Jun., 2007.

[13] D. Cribbs, M. Ellenberger, and J. Hassler, "self-servo writing disk drive and method," U.S. Patent 5448429, 1995.

[14] D. Abramovitch, T. Hurst, and D. Henze, "An overview of the PES Pareto method for decomposing baseline noise sources in hard disk position error signals," *IEEE Trans. On Magnetics*, vol. 34, no. 1, pp. 17-23, 1998.

[15] T. Ciftcibasi and O. Yuksel, "Sufficient or necessary conditions for modal controllability and observability of Roesser's 2-D system model," *IEEE Trans. On Automatic Control*, vol. AC-28, no. 4, pp. 527-529, 1983.

[16] H. N. Melkote, R. McNab, B. Cloke, and V. Agarwal, "A study of radial error propagation and self-servowriting in disk drives," in *Proceedings of 2002 American Control Conference*, 2002, pp. 1372-1377.

[17] C. Du, L. Xie, J. N. Teoh, and G. Guo, "H_2 Control for Head Positioning in Axial and Radial Dimensions for Self-Servo Track Writing," *IEEE Trans. on Control Systems Technology*, vol. 16, No. 1, pp. 177-181, January 2008.

[18] C. Du, L. Xie, and C. Zhang, "H_∞ control and robust stabilization of two-dimensional systems in Roesser models," *Automatica*, vol. 37, no. 2, pp. 205-211, 2001.

[19] R. Yang, L. Xie, and C. Zhang, "H_2 and robust H_2/H_∞ control of 2-D systems in Roesser model," *Automatica*, vol. 42, no. 9, Sept. 2006.

[20] C. Du, J. Zhang, and G. Guo, "Disturbance Modeling and Control Design for Self-Servo Track Writing," *IEEE Trans. On Mechatronics*, vol. 10, no. 1, pp. 122-127, Feb. 2005.

[21] S. Wu and M. Tomizuka, "An Iterative Learning Control Design for Self-Servowriting in Hard Disk Drives," *Proceedings of the 17th World Congress*, the IFAC, Seoul, Korea, July 6-11, 2008.

[22] F. Dong and M. Tomizuka, "An iterative learning control for self-servowriting in hard disk drives using L_1 optimal control," *Proceedings of the 2009 American Control Conference*, pp. 240-245, 2009.

[23] H. Melkote and R. J. McNab, "Modeling and control for self-servowriting in hard disk drives: A repetitive process approach," *Proceedings of the 2006 American Control Conference*, pp. 2005-2010, June 14-16, 2006.

[24] N. Nakamura, N. Bando, and Y. Hori, "Control design for self servo track writer using estimation of the head position," *9th IEEE International Workshop on Advanced Motion Control*, pp. 99-102, 2006.

[25] IEEJapan technical committee on Nano-Scale Servo (NSS) system. NSS homepage, 2006. URL http://mizugaki.iis.u-tokyo.ac.jp/nss/.

[26] J. Nie and R. Horowitz, "Design and Implementation of Dual-Stage Track-Following Control for Hard Disk Drives," *Proceedings of the 2nd Dynamic Systems and Control Conference*, Hollywood, California.

[27] J. C. Doyle, K. Glover, P. Khargonekar, and B. Francis, "State-space solutions to standard H_2 and H_∞ control problems," *IEEE Trans. on Automatic Control*, vol. 34, no. 8, pp. 831-847, August 1989.

[28] X. Chen and K. Zhou, "Multiobjective H_2/H_∞ Control Design", *SIAM J. Control Optim.*, vol. 40, No. 2, pp. 628-660, 2001.

[29] M. C. De Oliveira, J. C. Geromel, and J. Bernussou, "Extended H_2/H_∞ norm characterization and controller parametrizations for discrete-time systems," *Int. J. Control*, vol. 75, No. 9, pp. 666-679, 2002.